Rare Metal Materials and Engineering
Volume 48, Issue 8, August 2019
Available online at www.rmme.ac.cn

Science Press

Cite this article as: Rare Metal Materials and Engineering, 2019, 48(8): 2406-2412.

ARTICLE

Effect of Mechanical Milling Time on Helium Irradiation Behavior of W-Nb Alloys

Luo Laima[1,3], Xu Mengyao[1], Zan Xiang[1,3], Xu Qiu[4], Zhu Xiaoyong[1,3], Liu Jia-qin[2], Cheng Jigui[1,3], Wu Yucheng[1,3,5]

[1] School of Materials Science and Engineering, Hefei University of Technology, Hefei 230009, China; [2] Industry & Equipment Technology, Hefei University of Technology, Hefei 230009, China; [3] Laboratory of Nonferrous Metal Material and Processing Engineering of Anhui Province, Hefei 230009, China; [4] Kyoto University, Osaka-fu 590-0494, Japan; [5] National-Local Joint Engineering Research Centre of Nonferrous Metals and Processing Technology, Hefei 230009, China

Abstract: Mechanical milling can easily obtain nanopowders and consolidate milled powders to full density. Milling time exerts a critical influence on the performance of powders and bulk materials. In this study, the tungsten (W) combined with niobium (Nb) powder was wet milled for 15, 25, 36, and 45 h, and consolidated by spark plasma sintering. The W-Nb specimens were irradiated by 9.90×10^{24} ions m^{-2} helium (He) beams for 11 min. The results show that solid solution degree of W and Nb influences the irradiation damage of the specimen. The specimen milled for 36 h has the lowest solid solution degree, whose surface damage is the most serious among all specimens, and the nanostructure "fuzz" forms only in this specimen. In the same specimen, tungsten presents different surface damage degrees owing to its different orientations. After characterization, the W-Nb specimens were isochronally annealed at 900, 1100, and 1300 °C for 1 h. The grains grow in Nb-rich area but barely change in W-rich area, because Nb exerts a strong influence on the right shifting of He desorption peaks.

Key words: W-Nb alloys; mechanical milling; spark plasma sintering; helium irradiation; annealing

Tungsten (W) is a promising controllable plasma-facing material in nuclear fusion devices because of its superb properties, such as high melting point, sputtering threshold, and low tritium retention.

When W is bombarded by high fluxes of low-energy helium (He) particles and neutrons at high temperatures, its surfaces form a nanostructure called "W fuzz" at temperatures between 1000 and 2000 K, landing energies above 20 eV, and fluxes obviously higher than 2×10^{20} $m^{-2}\cdot s^{-1}$ [1,2]. These nanotendrils have been produced in linear plasma devices[3-5] and Alcator C-Mod[3,6]. The effect of fuzz on plasma-surface interaction mechanism and tokamak operations is still uncertain. However, the fuzz layers present low sputtering yield in bulk W[7] and are sensitive to uni-polar arcing[8].

W performance is restricted by inappropriate ductile-to-brittle transition temperatures. The ductility of W should be ameliorated to avoid thermal stress in fusion devices, which can be achieved by combining other ductile refractory metals[9]. Niobium (Nb) presents outstanding ductility in group V-B[10]. Niobium has a high melting point, corrosion resistance, and low thermal-neutron absorption cross-section. On the other hand, niobium has a high affinity for impurities such as O, C, and N, and can be bound with these impurity elements to form compounds with high melting temperatures, which can decrease the total retention D_2 and clean the grain boundary of W alloys. A small amount of niobium can improve the ductility of tungsten-based materials and alter their behaviors under irradiation.

Unlike wet chemical methods, mechanical milling can easily obtain nanopowders and consolidate the milled powders

Received date: August 24, 2018
Foundation item: National Magnetic Confinement Fusion Program (2014GB121001); National Natural Science Foundation of China (51474083); The Foundation of Laboratory of Nonferrous Metal Material Processing Engineering of Anhui Province (15CZS08031); "111" Project of China (B18018)
Corresponding author: Luo Laima, Ph. D., Professor, School of Materials Science and Engineering, Hefei University of Technology, Hefei 230009, P. R. China, Tel: 0086-551-62902604, E-mail: luolaima@126.com

Copyright © 2019, Northwest Institute for Nonferrous Metal Research. Published by Science Press. All rights reserved.

to full density[11]. Milling time exerts a critical influence on the performance of powders and bulk materials.

In addition, this paper tries to address questions that appear when tungsten is irradiated in high temperature environments found in fusion reactors. In order to understand the recovery behavior of displacement damage, quasi-in-situ annealing experiments were performed on tungsten-niobium samples followed by 50 eV He ion irradiation and subsequent hydrogen atmosphere annealing. The annealing temperatures ranged from 900 °C to 1300 °C. The annealing of bcc metals classified by Thompson[12] involves five stages. Stage I occurs below −170 °C due to the movement of free interstitials[13]. Stage II occurs at −170~350 °C, ascribed to the release of interstitials from trap with activation energies of 0.25~1.7 eV. The fusion reactor operates at 500~1000 °C[14]. The study of stages III~V is meaningful for first-wall materials. Stage III, with the temperature of ~350 °C/~0.15 T_m and activation energy of ~1.7 eV, is due to the monovacancy mobility activation[13]. Stage IV at 640 °C/0.22 T_m is ascribed to vacancy-impurity complex [14], or di-vacancy[15]. Stage V or the recovery stage at 0.31 T_m is due to vacancy migration[16] but that at high temperatures is attributed to the disappearance of defect cluster or formation of voids[17]. This experiment mainly occurs in stage V.

This experimental study aims to investigate the behavior of He-induced nanostructures in W-Nb alloys with different milling time.

1 Experiment

The powders used in this study contained 85 wt% pure W (>99.9%, 1.0~1.3 μm) and 15 wt% pure Nb (>99.9%, 40~50 μm), and were prepared by ball milling. Mechanical milling was performed in a planetary ball mill with a rotation speed of 400 r/min and a ball to powder ratio of 20:1 at room temperature, whose jar and ball were made of tungsten carbide (WC). The milling medium was absolute ethyl alcohol, and the milling time was 15, 25, 36, and 45 h. The powder was soaked in alcohol with air included in the pot. The powder was loaded in a graphite die with a diameter of approximately 20 mm. Then, DC current was applied to the pulse, and the high uniaxial mechanical pressure was obtained in this process. The prepared powders were consolidated by spark plasma sintering (LABOX™-350 spark plasma sintering system) at 1700 °C for 5 min. The specific sintering process is shown in Fig.1. The whole sintering process was carried out in vacuum. Chen[18] et al researched the microstructure and characteristic of this W-Nb alloy.

The W-Nb specimens with a dimension of 10 mm×10 mm×1 mm were mechanically polished with diamond polishing paste and irradiated with large-flux He^+ beams. The large-power materials irradiation experiment system was used to irradiate the W-Nb specimens. The incident He^+ energy was 50 eV, and the He^+ flux was 1.5×10^{22} ions $m^{-2}\cdot s^{-1}$ for 11 min.

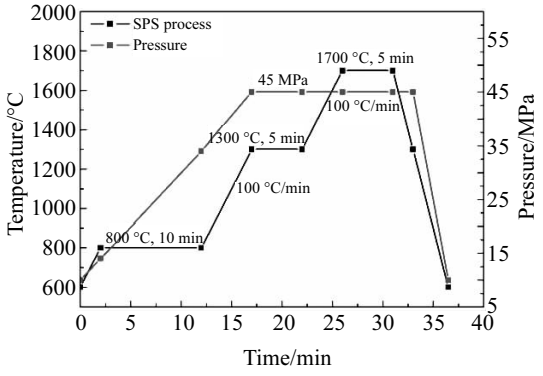

Fig.1 Specific sintering process of W-15wt%Nb alloys

The region directly irradiated by He^+ ions was a circle with a diameter of 7 mm. An infrared STL-150B pyrometer was installed outside the plasma in the ambient air to measure the specimen temperature. The surface temperature of W ranged between 1230~1280 K.

X-ray diffraction (XRD) with Cu Kα radiation was used to determine the phase change of the specimens in an X'pert PRO MPD machine after the irradiation. The change in surface microstructure was observed by field-emission scanning electron microscopy (FESEM). After characterization, the W-Nb specimens were isochronally annealed at 900, 1100, and 1300 °C for 1 h in hydrogen atmosphere to identify the damage recovery at different annealing temperatures. The change in surface morphologies was observed by FESEM.

2 Result and Discussion

Fig.2 shows the surface morphologies of non-irradiated specimens at different milling time. Porosity was observed in all alloys (Fig.2a, 2c and 2d; marked by arrow B in Fig.2a) except for the W-15wt%Nb alloy after 25 h of milling (Fig.2b). The result is consistent with the density shown in Table 1. The second phase particles in Nb-rich regions (marked by arrow A and shown by the inset of EDS spectrum in Fig.2a) are dispersed at the boundaries and within the grains. It can be seen in Fig.2b that the Nb-rich phase particles are homogenously distributed in the tungsten grains and boundaries of the W-Nb alloy after 25 h of milling, because the powder size of 25 h milled sample is small (Table 1). As the milling time increases from 15 h to 25 h, the size of particle decreases and it tends to be flat, which is beneficial to sintering. The sample after 25 h milling has a higher density and a smaller grain size. When the milling time was extended to 36 h, the agglomeration of the fine Nb phase started. After sintering, the reuniting of Nb-rich region was observed. However, after the milling time reached 45 h, the large-sized layer of Nb-rich regions was ruptured and redistributed in the tungsten boundary.

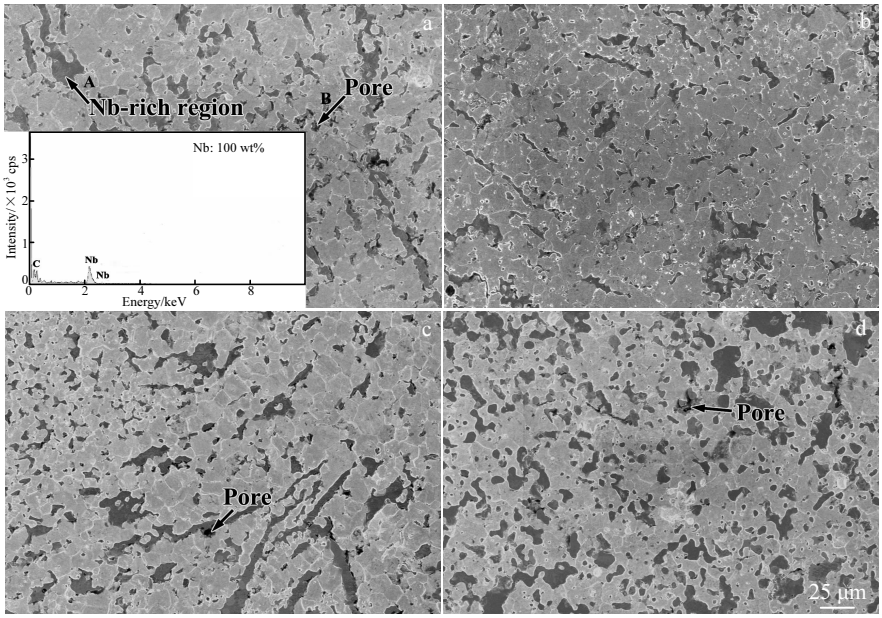

Fig.2 SEM images of non-irradiated specimens with different milling time: (a) 15 h, (b) 25 h, (c) 36 h, and (d) 45 h

Table 1 Density and grain size of W-Nb alloys with different milling time

Time/h	Density/%	Grain size/μm
15	95.5	3~8
25	98.1	3~5
36	97.2	3~8
45	96.6	3~7

Fig.3 shows the SEM images of irradiated W-Nb alloys with milling time of 15, 25, 36, and 45 h at a flux of 1.50×10^{22} He^{+} $m^{-2}\cdot s^{-1}$ at 1255 °C. Milling time exerts a strong influence on surface morphology. The EDS spectrum (inset in Fig.3b) shows that the porous regions pointed by the arrows are Nb-rich regions. The W-rich regions exhibit several different morphologies in all milling time and are highly orientation dependent. Parish et al[19] conducted the relevant research. The normal-direction orientation of the grains controls the growth morphology. In particular, pyramids are formed by near-<011>∥normal direction (ND) grains, wavy and stepped structures are formed by near-<114> to <112>∥ ND grains, and smooth morphologies are formed by near-<103>∥ ND grains. In Fig.3a, the smooth, pyramidal, terrace, and wavy morphologies are marked by I~IV, respectively. The differences among the three orientations are attributed to the ion channeling, surface energy, and dislocation loop-punching effects. These theories cannot explain the difference in surface morphologies in all directions, so a comprehensive theoretical study is required. The different surface morphologies are in the early stages of fuzz growth. The nanostructure formation is due to the trap mutation mechanism[20-24]. The aggregation of several He atoms moves the W atom from the original lattice position, thereby forming a Frenkel pair. The vacancy attracts He atoms to form a He-vacancy complex as an immobile embryo of He bubbles. The strong interactions among He atoms form the He clusters. Finally, helium nanobubbles grow rapidly and push the surface up. Then, the migration of He expands the He cluster. When He bubbles are too large, the internal pressure becomes too high and then surface cracks, thereby forming the nanofuzz[25,26]. Meanwhile, the grain boundaries act as strong traps rather than fast diffusion paths[26]. This phenomenon explains why the fuzz easily forms at grain boundary. The ellipses in Fig.3a, 3b and 3d show that the fuzz easily forms at the interface between W and Nb. The regions near the W-Nb boundaries serve as strong traps, aggregating a large number of He atoms. This condition results in a lot of helium bubbles and a large amount of cavities, thereby forming the fuzz.

The arrows in Fig.3 refer to the Nb-rich regions. Notably, the morphology of Nb-rich regions is very different from that of W-rich regions. In particular, the Nb-rich regions present mostly porous surface morphology. The nanofuzz structure is formed in the W-rich regions whereas not formed in the Nb-rich regions. Interstitial formation energy of the helium in niobium is much smaller than that in tungsten. In other words, helium ions exist in niobium more easily[27]. The dissolution and diffusion of helium in niobium-doped tungsten were calculated by the first-principles electronic structure calculations[28]. Niobium in tungsten can serve as a helium trapping center and cause significant attraction to helium. The addition of niobium causes a difference in the charge density of tungsten,

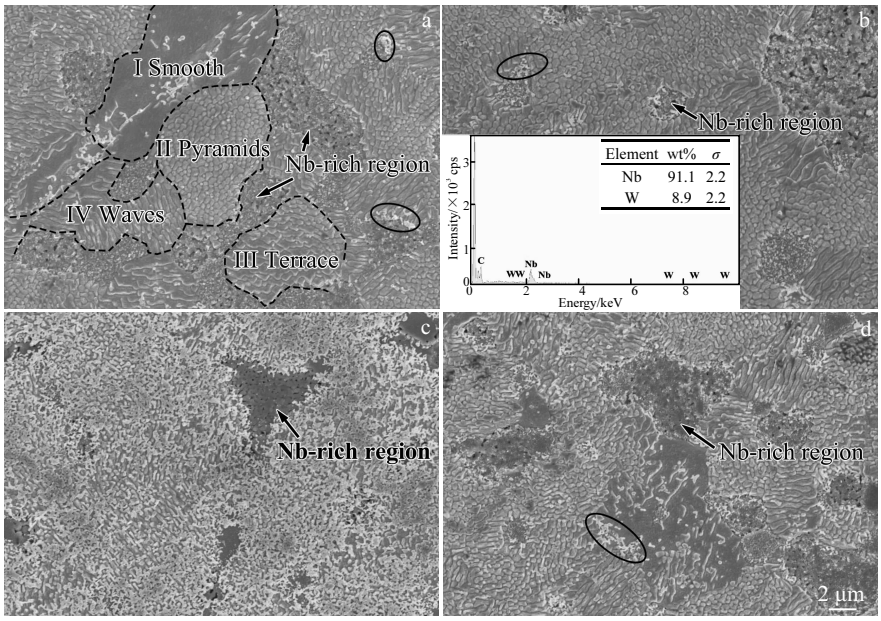

Fig.3 SEM images of the irradiated W-15wt%Nb alloys with different milling time at a flux of 1.5×10^{22} $m^{-2}\cdot s^{-1}$ at a temperature of approximately 1255 °C: (a) 15 h, (b) 25 h, (c) 36 h, and (d) 45 h

which makes the solubility of helium in the nearest niobium neighbors much lower than that in intrinsic tungsten. The diffusion barrier around niobium decreases gradually with increasing the distance between helium and niobium, indicating that helium is easily trapped by niobium. Therefore, the helium ions will preferentially accumulate in niobium, thereby protecting the matrix to a certain extent. According to Liu et al[29], the W specimens form fuzz structure at He^+ energies of 30 eV and He^+ flux of 1.6×10^{22} $m^{-2}\cdot s^{-1}$. Compared with this experiments result, the radiation resistance of Nb-doped tungsten was improved obviously.

The preliminary work shows that the W-Nb specimen milled for 25 h exhibits the highest relative density, smallest Nb-rich phase, and highest uniformity among all specimens[18]. Fig.3b is the maximum irradiation center area under the same irradiation condition. Fig.3c shows that the radiation resistance of the sample milled for 36 h is slightly worse than that of other samples. After the W-Nb specimens milled for 36 h are irradiated, a fuzz structure is observed in the surface. Fig.4 shows the XRD patterns of non-irradiated W-15wt%Nb alloys with different milling time. Nb_4C_3 is evident in the XRD pattern. The formation of the Nb_4C_3 is due to the transformation of WC phase which is introduced by the ball milling and the carbon pollution during the SPS. Among them, carbon pollution during the SPS sintering is the main source. Compared with the diffraction peak of standard tungsten, the peak position of W shifts to lower angles in the XRD pattern of all W-Nb alloys, except for the alloy with 36 h milling. The left shifting of W phase is due to the formation of W (Nb) solid solution. The previous analysis shows that the diffusion of He into Nb is greater than that into tungsten. The formation of W (Nb) solid solution makes it easy for Nb-rich region to concentrate the helium ions in tungsten and to reduce the damage of tungsten exposed to helium irradiation. Therefore, numerous voids form in the Nb-rich region of the sample milled for 15, 25, and 45 h, as shown in Fig.5a, 5b and 5d. The damage of Nb-rich region is more severe than that of the W-rich region. However, the W peak of the sample with 36 h ball milling does not shift to the left obviously, which may be due to the particle agglomeration. The W-rich region of the alloy with 36 h milling forms a fuzz structure, and the damage in Nb-rich region is significantly better than that of other samples (Fig.5c). Eventually, it leads to the accumulation of helium ions in the W-rich region, resulting in the formation of fuzz.

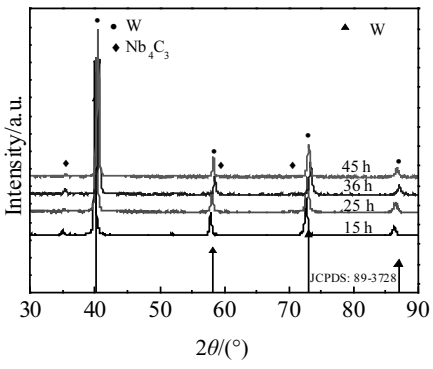

Fig.4 XRD patterns of non-irradiated W-15wt%Nb alloys with different milling time

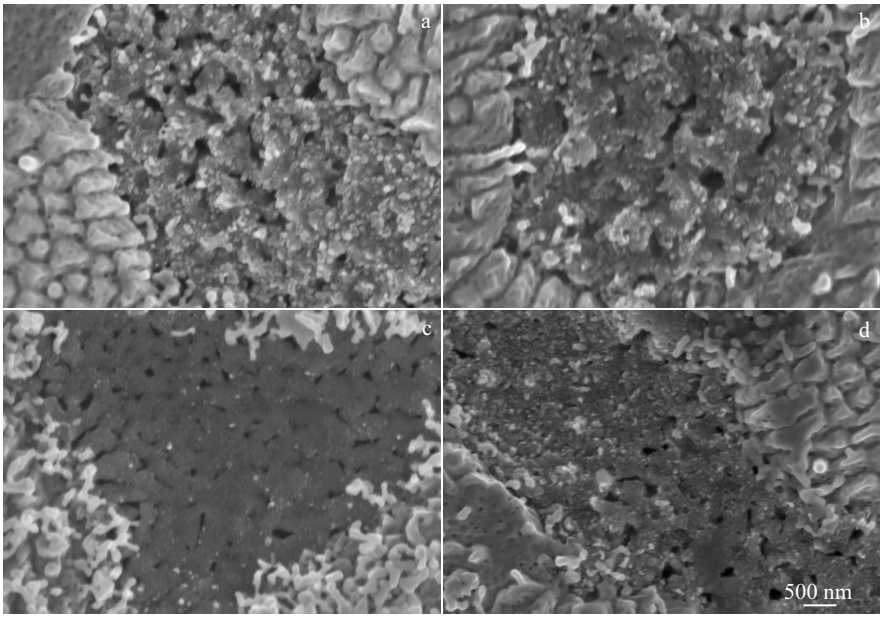

Fig.5 Highly magnified SEM images of niobium-rich region of irradiated W-15wt%Nb alloys with different milling time: (a) 15 h, (b) 25 h, (c) 36 h, and (d) 45 h

After irradiation, the sample with a milling time of 45 h was selected, whose performance was moderate and not much peculiar. The sample was annealed isochronally at 900, 1100, and 1300 °C for a fixed time. The surface morphology of the sample was observed at different annealing temperatures. This experiment aims to investigate the behavior of radiation damage repair in high-temperature environments found in fusion reactors. Fig.6 shows the quasi-in-situ SEM images of surface changes at different annealing temperatures. Fig.6a shows the image of the sample without annealing, and Fig.6b, 6c, and 6d show the images of the samples annealed at 900, 1100, and 1300 °C, respectively. As shown in Fig.6, the Nb-rich phase presents a significant grain growth whereas the W-rich phase exhibits no obvious grain change. No significant change is observed in W and Nb at the annealing temperature of 900 °C (Fig.6b). The grain sizes of Nb-rich phase enlarge,

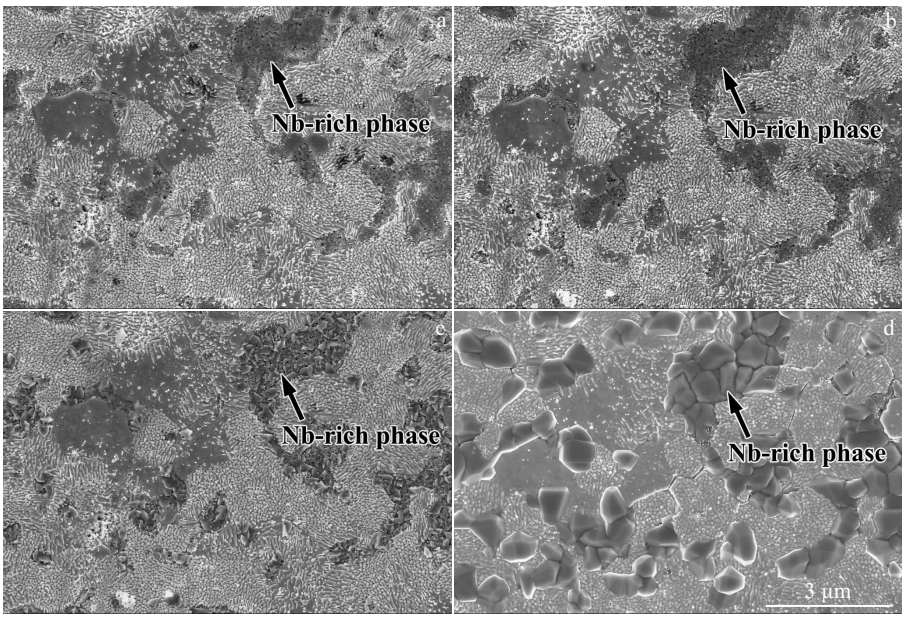

Fig.6 SEM images of the W-15wt%Nb alloys isochronally annealed at different temperatures for 1 h: (a) unannealed, (b) 900 °C, (c) 1100 °C, and (d) 1300 °C

and some pores in Nb-rich phase are combined at 1100 °C. Meanwhile, the morphology of W-rich phase is the same as that of unannealed one. The grains grow abnormally and the pores are completely repaired in the Nb region at 1300 °C. The abnormal growth of Nb in some areas causes surface cracks. At the same time, the fuzz at the W-Nb interface disappears completely, and the morphologies of terraced W surface at other locations are slightly eliminated. Ferroni et al[30] investigated the effect of annealing on the dislocation density of irradiated W, and found that with the increase in temperature, the loop number density decreases whereas the mean dislocation loop diameter increases. At 1400 °C, dislocation loop completely disappears. In the current study, Nb is constantly recovered at stage V. At 900 °C, the vacancies in Nb-rich region migrate and macroscopically show that small voids merge into large pores. At 1300 °C, the Nb-rich region is completely repaired internally and the excess energy causes the recrystallization of Nb. Meanwhile, the morphology of W-rich phase barely changes. The possible reason for this phenomenon is that the addition of Nb allows for the right shifting of He desorption peaks. Baldwin et al [21] explored the effect of various W grades on the "fuzz" nanostructure formation. The results show that the desorption peak of He in W alloys appears at 770, 1170, and 1530 °C, and is higher than that of the general experiment. Nb has high affinity for impurities (such as O, C, and N) and can be bound with those impurity elements to form compounds with high melting temperatures, which can clean the grain boundary of W alloys[31]. The compound formed by the combination of niobium and impurities has the effect of pinning the grain boundary and preventing grain growth. If the dislocations are induced to slip, they must overcome the pinning effect. The incorporation of Nb will also change the elastic modulus of W, diffusion coefficient, and cohesion. The dislocation lines are bent, and the resistance to dislocation slip increases. Thus, the recovery temperatures of W become higher. However, further experiments are needed to prove our conjecture.

3 Conclusions

1) Milling time has a strong influence on the surface morphology of W-Nb alloy. The surface damage of the specimen milled for 36 h is serious, and the "fuzz" nanostructure forms only in this specimen. The solid solution degree of W and Nb influences the irradiation damage of the specimen.

2) In the same specimen, W shows different surface damage degrees owing to its different orientation. The fuzz easily forms in the interface between W and Nb.

3) After isochronal annealing, the grain of Nb-rich area grows whereas it barely changes in W-rich area. Nb exhibits a strong influence on the right shifting of He desorption peaks.

References

1 Fiflis P, Curreli D, Ruzic D N. *Nucl Fusion*[J], 2015, 55: 33 020

2 Luo L M, Tan X Y, Chen H Y *et al*. *Powder Technol*[J], 2015, 273: 8

3 Wright G M, Brunner D, Baldwin M J *et al*. *J Nucl Mater*[J], 2013, 438: S84

4 Takamura S C, Ohno N, Nishijima D *et al*. *Plasma Fusion Res*[J], 2006, 1: 51

5 Lee G, McKittrick J, Ivanov E *et al*. *Int J Refract Met Hard Mater*[J], 2016, 61: 22

6 Wright G M, Brunner D, Baldwin M J *et al*. *Nucl Fusion*[J], 2012, 52: 42 003

7 Nishijima D, Baldwin M J, Doerner R P *et al*. *J Nucl Mater*[J], 2011, 415(1): S96

8 Kajita S, Takamura S C, Ohno N. *Nucl Fusion*[J], 2009, 49: 32 002

9 Rieth M, Boutard J L, Dudarev S L. *J Nucl Mater*[J], 2011, 417(1-3): 463

10 Mateus R, Dias M, Lope J *et al*. *J Nucl Mater*[J], 2013, 438: S1032

11 Sarwat S G. *Powder Metall*[J], 2017, 60(4): 267

12 Thompson M W. *Philos Mag*[J], 1960, 5(51): 278

13 Mason D R, Yi X, Kirk M A. *J Phys Condens Mat*[J], 2014, 26: 375 701

14 Bykov V N, Birzhevoi G A, Zakharova M I *et al*. *Soviet Atomic Energy*[J], 1972, 33: 930

15 Zakharova M I, Solov'Ev V A, Bykov V N. *Soviet Atomic Energy*[J], 1975, 38: 101

16 Jeannotte D, Galligan J M. *Phys Rev Lett*[J], 1967, 19: 232

17 Dubinko A, Terentyev D, Bakaeva A *et al*. *Int J Refract Met Hard Mater*[J], 2017, 66: 105

18 Chen J B, Luo L M, Lin J S *et al*. *J Alloys Compd*[J], 2017, 694: 905

19 Parish C M, Hijazi H, Meyer H M *et al*. *Acta Mater*[J], 2014, 62: 173

20 Wang K, Bannister M E, Meyer F W *et al*. *Acta Mater*[J], 2017, 124: 556

21 Baldwin M J, Doerner R P. *J Nucl Mater*[J], 2010, 404: 165

22 Wang J, Niu L L, Shu X L *et al*. *J Phys Condens Mat*[J], 2015, 27: 395 001

23 Hu L, Hammond K D, Wirth B D *et al*. *J Appl Phys*[J], 2015, 118: 163 301

24 Hu L, Hammond K D, Wirth B D *et al*. *J Appl Phys*[J], 2014, 115: 173 512

25 Tan X Y, Luo L M, Chen H Y *et al*. *Sci Rep*[J], 2015, 5: 12 755

26 Fiflis P, Curreli D, Ruzic D N. *Nucl Fusion*[J], 2015, 55: 33 020

27 Seletskaia T, Osetsky Y, Stoller R E *et al*. *Phys Rev B*[J], 2008, 78: 134 103

28 Wang X X, Zhang Y, Zhou H B *et al*. *Acta Phys Sin*[J], 2014, 63: 234

29 Liu L, Liu D P, Hong Y *et al*. *J Nucl Mater*[J], 2016, 471: 1

30 Ferroni F, Yi X O, Arakawa K. *Acta Mater*[J], 2015, 90: 380

31 Kharchenko V K, Bukhanovski V V. *Strength Mater*[J], 2012, 44: 512

机械球磨时间对 W-Nb 合金氦辐照行为的影响

罗来马[1,3]，徐梦瑶[1]，昝 祥[1,3]，徐 虬[4]，朱晓勇[1,3]，刘家琴[2]，程继贵[1,3]，吴玉程[1,3,5]

(1. 合肥工业大学 材料科学与工程学院，安徽 合肥 230009)

(2. 合肥工业大学 工业与装备技术学院，安徽 合肥 230009)

(3. 安徽省有色金属材料及加工工程实验室，安徽 合肥 230009)

(4. 京都大学，大阪府 590-0494)

(5. 有色金属与加工技术国家联合工程研究中心，安徽 合肥 230009)

摘 要：采用不同球磨时间制备 W-Nb 复合粉末，并通过放电等离子烧结方法制备 W-Nb 复合材料。所得的 W-Nb 复合材料用剂量为 9.90×10^{24} ions m^{-2} 的氦离子束辐照 11 min，随后分别在 900、1100 和 1300 ℃下热处理 1 h。结果表明，球磨时间不同导致复合材料中钨-铌固溶程度不同，进而造成了材料抗辐照损伤性能的差异。其中，球磨 36 h 的试样固溶程度最低，在辐照后其表面损伤也最严重，表面出现了纳米绒毛状结构。在同一个样品中，钨不同晶面取向也导致了不同的表面损伤形貌。通过对比不同热处理温度的试样，发现富铌区域的晶粒发生了明显的长大，但富钨区域的表面形貌几乎没有变化，这是由于铌的加入使得 He 在钨中的解吸峰右移。

关键词：W-Nb 合金；机械球磨法；放电等离体子烧结；氦辐照；热处理

作者简介：罗来马，男，1980 年生，博士，教授，合肥工业大学材料科学与工程学院，安徽 合肥 230009，电话：0551-62902604，E-mail: luolaima@126.com